

## Exploring the structure of Xe isotopes in $A \sim 130$ region: Single particle and collective excitations

R. Banik<sup>1,2,\*</sup>, S. Bhattacharyya<sup>1,2</sup>, S. Biswas<sup>3</sup>, S. Bhattacharya<sup>1,2</sup>, G. Mukherjee<sup>1,2</sup>, S. Rajbanshi<sup>4</sup>, S. Dar<sup>1,2</sup>, S. Nandi<sup>1,2</sup>, S. Ali<sup>5,2</sup>, S. Chatterjee<sup>6</sup>, S. Das<sup>6</sup>, S. Das Gupta<sup>7</sup>, S. S. Ghugre<sup>6</sup>, A. Goswami<sup>5,2</sup>, D. Mondal<sup>1</sup>, S. Mukhopadhyay<sup>1,2</sup>, H. Pai<sup>5</sup>, S. Pal<sup>1</sup>, D. Pandit<sup>1</sup>, R. Raut<sup>6</sup>, P. Ray<sup>5,2</sup>, and S. Samanta<sup>6</sup>

<sup>1</sup>Variable Energy Cyclotron Centre, 1/AF Bidhannagar, Kolkata 700064, India.

<sup>2</sup>Homi Bhabha National Institute, Training School Complex, Anushaktinagar, Mumbai-400094, India.

<sup>3</sup>GANIL, CEA/DRF-CNRS/IN2P3, Bd Henri Becquerel, BP 55027, F-14076 Caen Cedex 5, France.

<sup>4</sup>Department of Physics, Presidency University, Kolkata 700073, India.

<sup>5</sup>Saha Institute of Nuclear Physics, Kolkata 700064, India.

<sup>6</sup>UGC-DAE CSR, Kolkata Centre, Kolkata 700098, India.

<sup>7</sup>Victoria Institution (College), Kolkata 700009, India.

**Abstract.** High and medium spin structures of  $^{130,131}\text{Xe}$  have been studied using  $\alpha$ -induced fusion-evaporation reaction and the Indian National Gamma Array (INGA) coupled with a digital data acquisition system. Various new band structures and near yrast levels of  $^{131}\text{Xe}$  have been established. The multipolarities of the observed transitions have been assigned on the basis of the DCO ratios and the polarization asymmetry measurements. Band structures based on 1-quasi-particle (qp), 3-qp configurations have been observed. A new Magnetic Rotational (MR) band based on 5-qp configuration has also been established in  $^{131}\text{Xe}$ . The MR band has been interpreted in terms of shears mechanism with principal axis cranking (SPAC) calculations. Shell Model calculations are carried out to describe the non yrast states of  $^{131}\text{Xe}$  above the  $11/2^-$  isomer. New excited states have also been identified in  $^{130}\text{Xe}$ , produced in the same reaction.

### 1 Introduction

The transitional nuclei in the  $A \sim 130$  region are of current interest to explore the variety of nuclear structures arising from interplay between the single particle and the collective degrees of freedom. The shape driving nature of the  $h_{11/2}$  orbital, available for both protons and neutrons, and the corresponding particle-hole interactions drag the nucleus towards various exotic shapes and structures. The role of the unique parity  $h_{11/2}$  orbital is thus important in inducing deformation to the system and having deformed band structures based on both one quasi-particle (qp) and multi qp configurations.

$^{131}\text{Xe}$  ( $Z = 54$ ,  $N = 77$ ) is one of the suitable candidate to study various band structures and interesting features of the nuclear shape in  $A \sim 130$ . Only one qp ( $\nu h_{11/2}$ ) band structure in  $^{131}\text{Xe}$  is known [1, 2], whereas, high spin band structures in  $^{125}\text{Xe}$  [3] and triaxial bands in  $^{129}\text{Xe}$  [4] have been reported. Availability of high- $j$   $h_{11/2}$  orbital for both proton particles and neutron holes makes  $^{131}\text{Xe}$  also a suitable candidate to exhibit Magnetic Rotation (MR) at high spin. Such MR band is reported in  $^{123}\text{Xe}$  [5] and described using the tilted axis configuration with  $\pi h_{11/2} \otimes \nu h_{11/2}$ . As one approaches the  $N = 82$  shell closure the MR band becomes favourable for its proximity to spherical shape. The lower spin states of  $^{131}\text{Xe}$  are generated from single par-

ticle excitations of four proton particles and five neutron holes (with respect to  $^{132}\text{Sn}$ ) in various available orbitals. The understanding of the configurations of these states helps us to explain the underlying nucleon-nucleon interactions. Thus  $^{131}\text{Xe}$  can be an interesting nuclei to study the various mechanisms of generation of angular momentum in a single nuclei. Population of  $^{131}\text{Xe}$  is difficult due to lack of stable target-projectile combinations. Previous spectroscopic studies on this nuclei were carried out from decay spectroscopy [6, 7], Coulomb excitations [8], ( $\alpha$ , 3n) [1] and ( $\alpha$ , n) [9] measurements. But these studies are limited by the detection system used. A recent study on  $^{131}\text{Xe}$  [2] reports only the extension of the yrast band to higher spin. But no detail information about the other high spin structures is available prior to the present study.

Xenon isotopic chain is also known for its shape change from  $\gamma$ -soft rotor to spherical one. The possible phase transition for the even- $A$  Xe isotopes can be described using E(5) symmetry, where the nucleus undergoes from spherical vibrator to  $\gamma$ -soft rotor. Clark *et al.* [10] has predicted that the E(5) symmetry can be investigated in  $^{128}\text{Xe}$ . The spectroscopic study on  $^{128}\text{Xe}$  [11] has indicated that  $^{130}\text{Xe}$  can possibly be a better candidate to look for such E(5) symmetry breaking. The structure of  $^{130}\text{Xe}$  was studied using Coulomb excitation in inverse kinematics [11] and (n, n') reaction [12], which concluded that this nucleus may not be the candidate for E(5) symmetry.

\*e-mail: ranabir.banik@vecc.gov.in

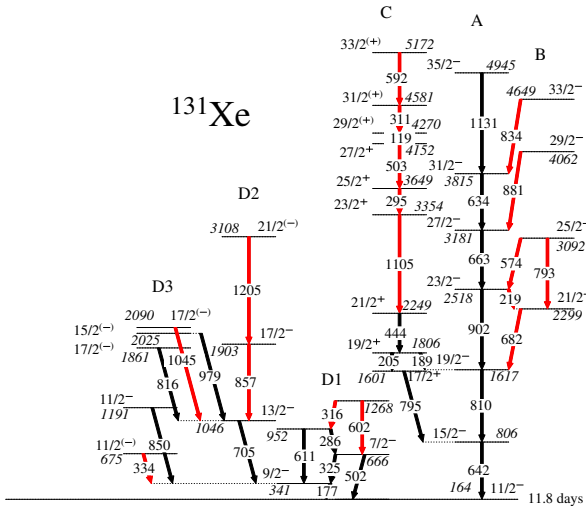


**Figure 1.** Partial level scheme of  $^{131}\text{Xe}$  as obtained in the present work. New  $\gamma$  ray transitions are marked with red colour.

But to know the detail low lying structures, it is worth to re-investigate the non-yrast and yrast states of  $^{130}\text{Xe}$ .

## 2 Experiment and Data Analysis

The excited states of  $^{130,131}\text{Xe}$  have been populated using the reaction  $^{130}\text{Te}(\alpha, xn)^{130,131}\text{Xe}$ , at a beam energy of 38 MeV, obtained from the K-130 Cyclotron at Variable Energy Cyclotron Centre (VECC), Kolkata, India. The Indian National Gamma Array (INGA) at VECC [13] consisting of seven Compton suppressed Clover HPGe detectors were used to detect the de-exciting  $\gamma$  rays. Four detectors of the array were at  $90^\circ$ , two detectors were at  $125^\circ$  and one detector was at  $40^\circ$  with respect to the beam direction. PIXIE based digital data acquisition system [14] was employed to record the time stamped LIST mode data in both singles ( $M_\gamma \geq 1$ ) and coincidence mode ( $M_\gamma \geq 2$ ).

The LIST mode data were sorted using the IUCPIX sorting programs [14] and further analysed using the RADWARE [15] and LAMPS [16] data analysis packages to construct the symmetric and angle-dependent  $E_\gamma - E_\gamma$  matrices and  $E_\gamma - E_\gamma - E_\gamma$  cube. In the present work, the multipolarities of the observed  $\gamma$  rays were determined from the Ratio of the Directional Correlation of the Oriented states ( $R_{DCO}$ ) measurements, as described in Ref. [17]. The parities of the excited states have been assigned from the polarization asymmetry measurements ( $\Delta_{asym}$ ). The measured values of the  $\Delta_{asym}$  give an idea about the electromagnetic nature of the decaying transition. The description of the method can be found in the Ref. [18].

## 3 Results

The existing level scheme of  $^{131}\text{Xe}$  is significantly extended with the placement of 72 new transitions from the current measurement. The details of this will be given in a forthcoming publication. The partial level scheme of

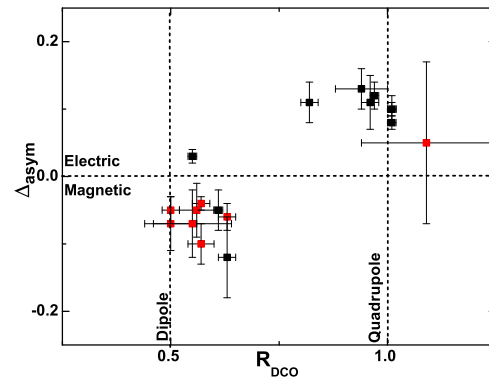


**Figure 2.** The DCO ratio ( $R_{DCO}$ ) [17] vs the polarization asymmetry ( $\Delta_{asym}$ ) [18] of the new  $\gamma$  rays (in red) reported in this work and that of the known  $\gamma$ -rays (in black). The DCO ratios are obtained in quadrupole gates. The dotted lines parallel to the Y-axis at 0.5 and 1.0 correspond to the DCO ratio of pure dipole and quadrupole transitions respectively. The dotted line parallel to the X-axis is to guide the eye for  $\Delta_{asym}$  values corresponding to the electric (+ve) and magnetic (-ve) nature of the transitions.

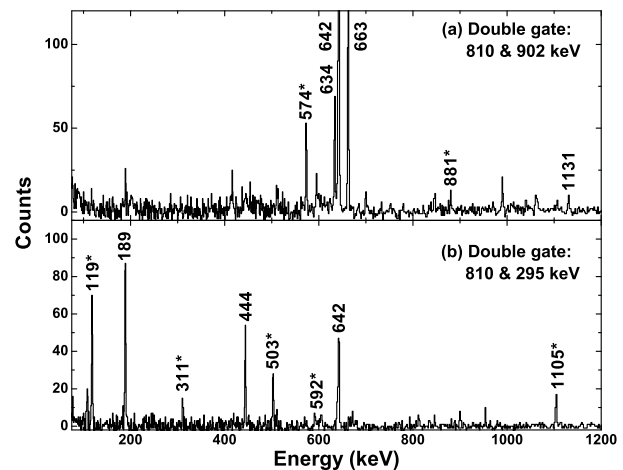


**Figure 3.** Spectra double gated on the (a) 810 - 902 keV and (b) 810 - 295 keV transitions of  $^{131}\text{Xe}$  from  $E_\gamma - E_\gamma - E_\gamma$  cube. Only the  $\gamma$  rays of interest of this paper are marked. The newly observed transitions are marked with '\*'.

$^{131}\text{Xe}$ , related to the present paper, is shown in Fig. 1. The  $R_{DCO}$  vs  $\Delta_{asym}$  plot for the transitions of  $^{131}\text{Xe}$ , reported in this paper are shown in the Fig. 2.

The main yrast negative parity band (Band A) of  $^{131}\text{Xe}$  is observed upto 4945 keV excitation energy as also observed by Kaya *et al.* [2]. The present work confirms the  $31/2^-$  (3814 keV) and  $35/2^-$  (4945 keV) spin assignments to the top two levels of this band, respectively, which could not be assigned in Ref. [2]. In the present work, a new band structure (Band B) ( $\Delta J = 2$ ) is identified, which decays to the main yrast band by M1 transitions of energy 682, 574, 881 and 834 keV. The M1 nature of these transitions are established from their deduced  $R_{DCO}$  and  $\Delta_{asym}$  values. This band B is the possible signature partner band of the main yrast sequence. Fig. 3(a) and (b) represent the coincidence spectra double gated on the 810 - 902 keV and

810 - 295 keV transitions respectively, from the  $E_\gamma$ - $E_\gamma$ - $E_\gamma$  cube. The presence of two different sets of new  $\gamma$  rays in these two spectra establishes another new band structure above 1617 keV level. The transitions of the main yrast band and the partner band are evident from Fig. 3(a). Fig. 3(b) shows another new set of  $\gamma$ -rays which are observed above the  $19/2^+$  state and are in coincidence with each other. This new band is extended upto 5172 keV,  $33/2^{(+)}$ , level with the observation of seven transitions and named with band C in the level scheme. Among these transitions, the 444 keV  $\gamma$ -ray was known from previous studies, but other transitions of energy 1105, 295, 503, 119, 311 and 592 keV are newly observed from the present work. The placement of these transitions are determined from their relative intensities. The deduced  $R_{DCO}$  values of  $\sim 0.5$  in a quadrupole gate along with negative  $\Delta_{asym}$  values establish these transitions as of M1 character.

Another set of new  $\gamma$ -rays are observed above the  $11/2^-$  state and parallel to the yrast band in  $^{131}\text{Xe}$ . Six new transitions of energies 316, 334, 602, 857, 1045 and 1205 keV are seen in the sequences D1, D2 and D3, which extends this part of the level scheme upto 3108 keV excitation.

As the yield of  $^{130}\text{Xe}$  is less at the beam energy chosen for the present reaction, only a limited set of data could be obtained on this nucleus. In this work, the main yrast structure in  $^{130}\text{Xe}$  is observed above the particle alignment. Various non-yrast states are also observed parallel to the main yrast structure in the  $^{130}\text{Xe}$ .

## 4 Discussion

The ground state of  $^{131}\text{Xe}$  is determined by the odd valence neutron. The lowest two levels of this nucleus are  $3/2^+$  (0 keV) and  $11/2^-$  (164 keV), which originate from the odd neutron occupying the available  $d_{3/2}$  and  $h_{11/2}$  orbitals. The large spin difference between these two states enforces the  $11/2^-$  state to be a long lived isomer (11.84 d) in  $^{131}\text{Xe}$ . This isomeric state decays to the  $3/2^+$  ground state by IT decay [19].

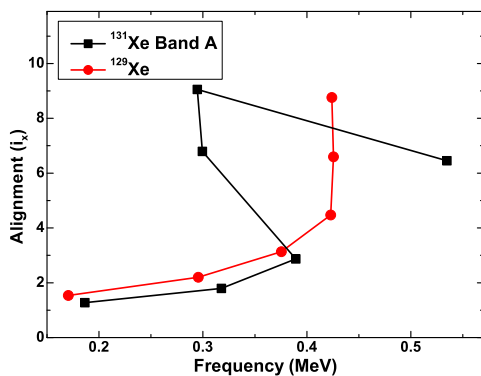


**Figure 4.** Alignment ( $i_x$ ) vs Frequency plot of the  $\nu h_{11/2}$  band in  $^{131}\text{Xe}$  and  $^{129}\text{Xe}$ .

The rotational structure built on the  $11/2^-$  state is reported in Kaya *et al.* [2] and also seen in this work. Fig. 4 represents the variation of single particle alignment as

function of rotational frequency for the yrast negative parity  $\nu h_{11/2}$  band (Band A) of  $^{131}\text{Xe}$  and  $^{129}\text{Xe}$ . Backbending with large alignment gain is observed for this band in  $^{131}\text{Xe}$ , whereas  $^{129}\text{Xe}$  shows an upbending. Such gain in alignment in  $^{131}\text{Xe}$  takes place due to the alignment of a pair of protons in  $h_{11/2}$  orbital. Band A and band B in  $^{131}\text{Xe}$  are found to have large staggering parameter, similar to its isotopic and isotonic partners. Large signature splitting as observed for this band indicates a large  $\Omega$  mixing.

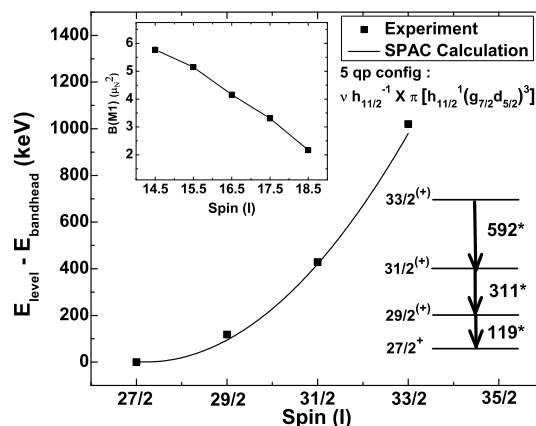


**Figure 5.** Level energy ( $E_{level}$ ) with respect to the band head energy ( $E_{bandhead}$ ) as a function of level spin which is compared with the SPAC calculation. The level sequence with the decaying  $\gamma$  rays are also shown. The inset shows the calculated  $B(M1)$  values using SPAC model as function of level spin.

The sequence of M1  $\gamma$ -rays (Band C) above the  $23/2^+$  state is connected to the  $21/2^+$  state by a relatively higher energy 1105 keV transition. This implies that these two parts have different configurations, with a 5-qp configuration to the upper part of the band (above  $27/2^+$ ) and a 3-qp configuration to the lower part. The upper part of this band is likely to have an extra pair of proton aligned which gives rise to a configuration  $\pi[(d_{5/2}g_{7/2})^3 h_{11/2}] \otimes \nu h_{11/2}^{-1}$ . This structure may possibly a MR band and thus discussed in the framework of Shears mechanism with the Principle Axis Cranking (SPAC) model [20–23]. The description of this theoretical model can be found in the Ref. [22]. For the present case, SPAC calculation is carried out considering the aforesaid configuration and assuming  $J_\pi = 12 \hbar$  and  $J_\nu = 5.5 \hbar$ . The level energies with respect to the band head energy as a function of level spin for the dipole band is plotted in the Fig. 5. Those experimental points are compared with the present calculation (solid line) and are found to be matching well. The calculated transition probabilities,  $B(M1)$ , are also plotted as a function of level spin and shown in the inset of Fig. 5. It is clearly seen from the figure, that the  $B(M1)$  values go on decreasing as the spin increases, which is one of the signature of magnetic rotational band. But a concrete evidence for this band to be a MR band would be an experimental observation of decreasing  $B(M1)$  values, which is out of the scope of the present experiment. Present SPAC model calculations also

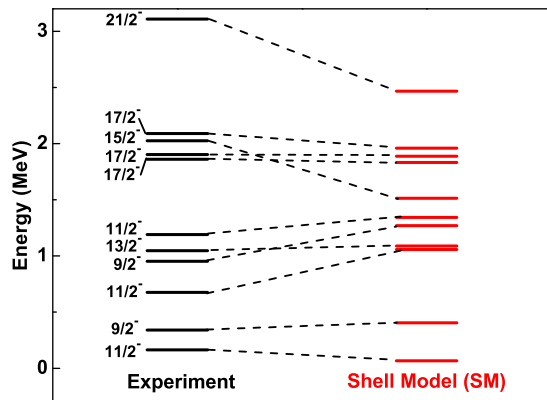


**Figure 6.** Comparison of the calculated energy levels (red) using shell model calculations with the experimental levels (black).

predicts that the 91% of the total angular momentum of the levels of this band is generated via shears mechanism.

The levels in the sequences, marked as D1, D2 and D3 in the level scheme (Fig. 1), are found to decay via various non-stretched transitions, indicating these states to be of single particle origin. Shell Model calculations are carried out for these states employing the code NUSHELLX [24] in the *gds* model space with the *jj55pna* Hamiltonian (referred as SN100PN interaction) [25]. The available orbitals consisting in the shell  $N, Z = 50 - 82$  are  $g_{7/2}$ ,  $d_{5/2}$ ,  $d_{3/2}$ ,  $s_{1/2}$  and  $h_{11/2}$  for both protons and neutrons. The calculations are carried out without any restriction in proton and neutron model space. The comparison between the calculated energy levels and the experimental levels of sequences D1, D2 and D3 are shown in Fig. 6. For this purpose, the experimental levels with increasing order of excitation energy for a given spin are compared with the corresponding states of shell model calculations. A good agreement between experimental states and shell model calculations for sequences D1, D2 and D3 are obtained.

## 5 Summary

The excited states in  $^{130,131}\text{Xe}$  have been studied using  $\alpha$ -induced fusion evaporation reaction and INGA detection setup. The existing level scheme of  $^{131}\text{Xe}$  is extended with the observation of signature partner band of the yrast band and a MR band. Other new set of low-lying levels above the  $11/2^-$  isomer are also observed. The MR band is discussed using SPAC model calculations and the non yrast states are interpreted in terms of Shell Model calculations.

## 6 Acknowledgements

The authors thank the staffs of the Accelerator group at VECC, Kolkata. The support from CEFIPRA Project No.

5604-4 is also thankfully acknowledged. R.B and S.N acknowledge the financial support received from the Department of Atomic Energy (DAE), Government of India.

## References

- [1] A. Kerek, A. Luukko, M. Grecescu *et al.*, Nucl. Phys A **172**, 603 (1971).
- [2] L. Kaya, A. Vogt, P. Reiter *et al.*, Phys. Rev. C **98**, 014309 (2018).
- [3] A. Al-Khatib, G. B. Hagemann, G. Sletten *et al.*, Phys. Rev. C **83**, 024306 (2011).
- [4] Y. Huang, Z. G. Xiao, S. J. Zhu *et al.*, Phys. Rev. C **93**, 064315 (2016).
- [5] G. Rainovski, D. L. Balabanski, G. Roussev *et al.*, Phys. Rev. C **66**, 014308 (2002).
- [6] R. A. Meyer, F. Mommyer and W. B. Walters, Z. Physik **268**, 387 (1974).
- [7] A. D. Irving, P. D. Forsyth, I. Hall *et al.*, J. Phys. G: Nucl. Phys. **5**, 1595 (1979).
- [8] D. C. Palmer, A. D. Irving, P. D. Forsyth *et al.*, J. Phys. G: Nucl. Phys. **4**, 1143 (1978).
- [9] T. Lönnroth, J. Kumpulainen and C. Tuokko, Physica Scripta. **27**, 228, (1983).
- [10] R. M. Clark, M. Cromaz, M. A. Deleplanque *et al.*, Phys. Rev. C **69**, 064322 (2004).
- [11] L. Coquard, N. Pietralla, T. Ahn *et al.*, Phys. Rev. C **80**, 061304(R) (2009).
- [12] E. E. Peters, T. J. Ross, S. F. Ashley *et al.*, Phys. Rev. C **94**, 024313 (2016).
- [13] Soumik Bhattacharya, R. Banik, S. Nandi *et al.*, DAE Symp. on Nucl. Phys. **63**, 1156 (2018).
- [14] S. Das, S. Samanta, R. Banik *et al.*, Nucl. Instrum. Meth. A, **893**, 138 (2018).
- [15] D. C. Radford, Nucl. Instrum. Meth. A, **361**, 297 (1995)
- [16] <http://www.tifr.res.in/~pell/lamps.html>
- [17] A. Krämer-Flecken, T. Morek, R. M. Lieder *et al.*, Nucl. Instrum. Methods Phys. Res. A **275**, 333 (1989).
- [18] K. Starosta, T. Morek, Ch. Droste *et al.*, Nucl. Instrum. Methods Phys. Res. A **423**, 16 (1999).
- [19] Yu. Khazov, I. Mitropolsky and A. Rodionov, Nucl. Data Sheet **107**, 2715 (2006).
- [20] S. Frauendorf, Rev. Mod. Phys. **73**, 463 (2001).
- [21] R. M. Clark and A. O. Macchiavelli *et al.*, Annu. Rev. Nucl. Part. Sci. **50**, 1 (2000).
- [22] S. Rajbanshi, Abhijit Bisoi, Somnath Nag, *et al.*, Phys. Rev. C **90**, 024318 (2014).
- [23] A. A. Pasternak, E. O. Lieder and R. M. Lieder, Acta Phys. Pol. **B 40**, 647 (2009).
- [24] B. A. Brown and W. D. M. Rae, Nucl. Data Sheets **120**, 115(2014).
- [25] B. A. Brown, N. J. Stone, J. R. Stone *et al.*, Phys. Rev. C **71**, 044317 (2005).